

Contrastive Learning for Debiased Candidate Generation in Large-Scale Recommender Systems

Chang Zhou* Jianxin Ma* Jianwei Zhang*
Jingren Zhou Hongxia Yang

Alibaba Group
{ericzhou.zc, jason.mjx, zhangjianwei.zjw}@alibaba-inc.com
{jingren.zhou, yang.yhx}@alibaba-inc.com

Abstract

Deep candidate generation (DCG) that narrows down the collection of relevant items from billions to hundreds via representation learning is essential to large-scale recommender systems [11]. Standard approaches approximate maximum likelihood estimation (MLE) through sampling for better scalability and address the problem of DCG in a way similar to language modeling. However, live recommender systems face severe unfairness of exposure with a vocabulary several orders of magnitude larger than that of natural language, implying that (1) MLE will preserve and even exacerbate the exposure bias in the long run in order to faithfully fit the observed samples, and (2) suboptimal sampling and inadequate use of item features can lead to inferior representations for the unfairly ignored items. In this paper, we introduce *CLRec*, a *Contrastive Learning* paradigm that has been successfully deployed in a real-world massive *RECommender* system, to alleviate exposure bias in DCG. We theoretically prove that a popular choice of contrastive loss is equivalently reducing the exposure bias via inverse propensity scoring, which provides a new perspective on the effectiveness of contrastive learning. We further employ a fixed-size queue to store the items’ representations computed in previously processed batches, and use the queue to serve as an effective sampler of negative examples. This queue-based design provides great efficiency in incorporating rich features of the thousand negative items per batch thanks to computation reuse. Extensive offline analyses and four-month online A/B tests demonstrate substantial improvement, including a dramatic reduction in the Matthew effect.

1 Introduction

Large-scale industrial recommender systems usually adopt a multi-stage pipeline, where the first stage, namely candidate generation, is responsible for retrieving a few hundred relevant entities from a billion scale corpus. Deep candidate generation (DCG) [11], a paradigm that learns entity vector representations to enable fast k-nearest neighbor retrieval [23], has become an essential part of many live industrial systems with its enhanced expressiveness and improved flexibility compared to traditional collaborative filtering based frameworks.

Typical large-scale DCG models [11, 14, 49, 26] regard the problem of identifying the most relevant items to the users as estimating a multinomial distribution traversing over all items for each user, conditional on the user’s past behaviors. Maximum likelihood estimation (MLE) is the conventional principle for training such models. Apparently, exact computation of the log likelihood, which requires computing softmax looping over a million- or even billion-scale collection of items, is computationally infeasible. Sampling is thus crucial to DCG. Among the various sampling strategies, sampled-softmax [5, 21] usually outperforms the binary-cross-entropy based approximations such as NCE [15] and negative sampling [31].

However, the MLE paradigm and the sampling strategies mainly stem from the language modeling community, where the primary goal is to faithfully fit the observed texts. Indeed, live recommender systems are different from natural language texts in several aspects. Firstly, the training data are collected from current undergoing systems that might be sub-optimal and biased towards popular items. In such situations, some high-quality items can be under-explored in the training data, while an algorithm trained

*Equal contribution.

via MLE will continue to under-estimate the relevance of the under-explored items in order to faithfully fit the observed data. Secondly, the set of items for recommendation is much larger than the vocabulary of natural languages, e.g. $\approx 100M$ items in our system compared to $\approx 100k$ words. Many items may never be sampled in an epoch.

In this paper, we introduce *CLRec*, a practical *Contrastive Learning* framework for debiased DCG in *RECommender* systems. We establish the theoretical connection between contrastive learning and inverse propensity weighting, where the latter is a well-studied technique for bias reduction [33, 20, 39]. Our theoretical result complements the previous studies of contrastive learning [32]. We then present an easy-to-implement efficient framework to practically reduce the exposure bias of a large-scale system based on the theoretical result. In particular, our implementation maintains a fixed-size first-in first-out (FIFO) queue [16] to accumulate positive samples and their representations from the previous batches, and use the content of the queue to serve as the negative samples to be discriminated from the positive samples of the next batch. It guarantees that all items will be sampled sometime in an epoch to serve as the negative examples. More importantly, it allows us to reuse the computed results from the previous batches, e.g., saving 90% computation cost when the queue size is $10\times$ of the batch size. As a result, we can afford to encode complex features of the negative samples even when the negative sample size, i.e., the queue size, is very large, where the complex features may improve the quality of the learned representations of the under-explored items.

CLRec has been fully deployed into our live system as the default choice to serve billions of page views each day since February 2020. We observe that CLRec is capable of recommending high-quality items that are largely neglected by most current on-going systems, and it consistently outperforms the previous state-of-art baselines regarding the online recommendation performance.

2 The Proposed Framework

In this section, we prove the connection between contrastive learning and inverse propensity weighting (IPW), based on which we propose a practical framework for bias reduction in large-scale DCG.

2.1 Problem Formulation

Notations Given a dataset of user clicks $\mathcal{D} = \{(x_{u,t}, y_{u,t}) : u = 1, 2, \dots, N, t = 1, 2, \dots, T_u\}$, where $x_{u,t} = \{y_{u,1:(t-1)}\}$ represents a user's clicks prior to the t th click $y_{u,t}$, and T_u denotes the number of clicks from the user u . We will drop the sub-scripts occasionally and write (x, y) in place of $(x_{u,t}, y_{u,t})$ for conciseness. We use \mathcal{X} to refer to the set of all possible click sequences, i.e. $x \in \mathcal{X}$. Each $y \in \mathcal{Y}$ represents a clicked item, which includes various types of features associated with the item, while \mathcal{Y} is the set of all possible items. The features of y could be in any form, e.g., the item's unique identifier number, embeddings or raw data of its image and text description. The number of items $|\mathcal{Y}|$ easily reaches 100 million in large live systems.

Deep Candidate Generation The deep candidate generation paradigm involves learning a user behavior encoder $f_\theta(x) \in \mathbb{R}^d$ and an item encoder $g_\theta(y) \in \mathbb{R}^d$. The set of parameters used by each encoder is a subset of θ , i.e. the set of all trainable parameters in the system. It then takes $\{g_\theta(y)\}_{y \in \mathcal{Y}}$ and builds a k-nearest-neighbor search service, e.g., Faiss [23]. As a result, given an arbitrary user behavior sequence x at serving time, we can instantly retrieve the top k items relevant to the user by finding the top k candidate $g_\theta(y)$ similar to $f_\theta(x)$. Most implementations use inner product $\phi_\theta(x, y) = \langle f_\theta(x), g_\theta(y) \rangle$ or cosine similarity as the similarity score. The typical learning procedure fits the data following the maximum likelihood estimation (MLE) principle:

$$\arg \min_{\theta} \frac{1}{|\mathcal{D}|} \sum_{(x,y) \in \mathcal{D}} -\log p_\theta(y | x), \quad \text{where } p_\theta(y | x) = \frac{\exp \phi_\theta(x, y)}{\sum_{y' \in \mathcal{Y}} \exp \phi_\theta(x, y')}. \quad (1)$$

The denominator of $p_\theta(y | x)$ sums over all possible items, which is infeasible in practice and thus requires approximation, e.g., via sampling. However, the observed clicks for training are from the previous version of the recommender system. The training data thus suffer from exposure bias (i.e. missing not at random [34]) and reflect the users' preference regarding the recommended items rather than all potential items. High-quality items that have few clicks in the training data will likely remain under-recommended by a new algorithm trained via the MLE paradigm.

2.2 Understanding Contrastive Learning from a Bias-Reduction Perspective

We now introduce the family of contrastive losses that we are interested in, and reveal their connection with the inverse propensity weighting (IPW) [33, 20, 39] techniques for bias reduction.

Sampled Softmax The kind of contrastive loss we will investigate is strikingly similar to sampled softmax. We thus recap sampled softmax here and will show that the minor difference is crucial later. There are many variants of sampled softmax [5, 21], among which the following variant is integrated by TensorFlow [1] and popular for industrial systems:

$$\arg \min_{\theta} \frac{1}{|\mathcal{D}|} \sum_{(x,y) \in \mathcal{D}} -\log \frac{\exp(\phi_{\theta}(x, y) - \log q(y | x))}{\exp(\phi_{\theta}(x, y) - \log q(y | x)) + \sum_{i=1}^L \exp(\phi_{\theta}(x, y_i) - \log q(y_i | x))}, \quad (2)$$

where $\{y_i\}_{i=1}^L$ are L negative samples drawn from a pre-defined proposal distribution $q(y | x)$. Subtracting $\log q(y | x)$ is necessary for it to converge to the same solution as the exact loss in Eq. (1). Most implementations assume $q(y | x) = q(y)$ and set $q(y)$ somehow proportional to the popularity of the items to improve convergence. In practice, we would draw thousands of negative samples to pair with each positive example. Sampled softmax in general outperforms other approximations such as NCE [15] and negative sampling [31] when the vocabulary is large [30, 27, 11, 21].

Contrastive Loss We study the following type of contrastive loss [35, 32]:

$$\arg \min_{\theta} \frac{1}{|\mathcal{D}|} \sum_{(x,y) \in \mathcal{D}} -\log \frac{\exp(\phi_{\theta}(x, y))}{\exp(\phi_{\theta}(x, y)) + \sum_{i=1}^L \exp(\phi_{\theta}(x, y_i))}, \quad (3)$$

where $\{y_i\}_{i=1}^L$ are again sampled from $q(y | x)$ for each x to pair with the positive sample. It no longer optimizes the MLE loss in Eq. (1), because it misses $-\log q(y | x)$ and thus does not correct the bias introduced by sampling. Many efforts on contrastive learning have been focusing on designing a well-performing proposal distribution $q(y | x)$ [35, 8]. InfoNCE [32] demonstrates that this loss maximizes a lower bound of the mutual information between x and y if we set the proposal distribution $q(y | x)$ to be the actual data distribution $p_{\text{data}}(y)$, i.e. if we sample y proportional to its frequency in the dataset.

Contrastive Learning and Exposure Bias Reduction The contrastive loss as shown above in Eq. (3) has recently achieved remarkable success in various fields, e.g., visual representation learning [16]. Nevertheless, it still remains a question why the loss is effective. We will reveal that the contrastive loss is a sampling-based approximation of an inverse propensity weighted (IPW) loss. The IPW loss¹, whose derivation can be found in Section A of the supplemental material, is:

$$\arg \min_{\theta} \frac{1}{|\mathcal{D}|} \sum_{(x,y) \in \mathcal{D}} -\frac{1}{q(y | x)} \cdot \log p_{\theta}(y | x), \quad (4)$$

where $q(y | x)$ should be the propensity score function, which represents the probability that item y is recommended to user x when we were collecting the training data \mathcal{D} . The idea of IPW is to model missing-not-at-random via the propensity scores in order to correct the exposure bias. We provide a proof in Section A of the supplemental material that the IPW loss is optimizing $p_{\theta}(y | x)$ to capture the oracle user preference even when there exists exposure bias. A standard implementation of the IPW loss has two steps, where the first step is to use a separate model to serve as $q(y | x)$ and optimize it by fitting the exposure history according to the MLE principle, while the second step is to optimize $p_{\theta}(y | x)$ according to Eq. (4). However, the two-stage pipeline of IPW, as well as the numerical instability brought by $\frac{1}{q(y|x)}$, makes IPW impractical for large-scale production systems.

Fortunately, we can prove that the contrastive loss Eq. (3) is in principle optimizing the same loss as Eq. (4). And in Subsection 2.3 we provide a simple implementation that does not require two separate steps and avoids the instability from the division of $q(y | x)$. Our key theoretical result is as follows:

¹Note that our IPW loss is different from the previous works on debiased recommenders [34, 43]. We focus on *multinomial* propensities, i.e. whether an item is selected and recommended by a recommender out of all possible items. The previous works consider *bernoulli* propensities related with users' attention, i.e. whether a user notices a recommended item or not, and mostly deal with the position bias in ranking.

Theorem 1. *The optimal solutions of the contrastive loss (Eq. 3) and the IPW loss (Eq. 4) both minimize the KL divergence from $p_\theta(y | x)$ to $r(y | x) = \frac{p_{\text{data}}(y|x)/q(y|x)}{\sum_{y' \in \mathcal{Y}} p_{\text{data}}(y'|x)/q(y'|x)}$. Here $p_{\text{data}}(y | x)$ is the data distribution, i.e. what is the frequency of y appearing in \mathcal{D} given context x .*

Proof. We now give a proof sketch on the theorem. We will focus on one training instance, i.e. one sequence $x \in \mathcal{X}$. The IPW loss (Eq. 4) for training sample x is $-\sum_{y:(x,y) \in \mathcal{D}} \frac{1}{q(y|x)} \log p_\theta(y | x) \propto -\sum_{y \in \mathcal{Y}} \frac{p_{\text{data}}(y|x)}{q(y|x)} \log p_\theta(y | x) \propto -\sum_{y \in \mathcal{Y}} r(y | x) \log p_\theta(y | x) = D_{\text{KL}}(r \| p_\theta) + \text{const. w.r.t. } \theta$. The IPW loss is thus minimizing the Kullback–Leibler (KL) divergence from $p_\theta(y | x)$ to $r(y | x)$.

Let us now focus on the contrastive loss for the training sample (x, y) . Let $C = \{y\} \cup \{y_i\}_{i=1}^L$, where y is the positive example and $\{y_i\}_{i=1}^L$ are the L negative samples drawn from $q(y | x)$. Note that C is a multi-set where we allow the same item to appear multiple times. The contrastive loss (Eq. 3) for x equals to $-\sum_{y:(x,y) \in \mathcal{D}} \sum_C q(C | x, y) \log \frac{\exp(\phi_\theta(x, y))}{\sum_{y' \in C} \exp(\phi_\theta(x, y'))} \propto -\sum_{y \in \mathcal{Y}} \sum_C q(C | x, y) p_{\text{data}}(y | x) \log \frac{\exp(\phi_\theta(x, y))}{\sum_{y' \in C} \exp(\phi_\theta(x, y'))}$, where $q(C | x, y) = \prod_{i=1}^L q(y_i | x)$ if $y \in C$ or $q(C | x, y) = 0$ if $y \notin C$, since by definition C must include y if we know that the positive example is y .

Let $q(C | x) = \prod_{y' \in C} q(y' | x)$. We then have $q(C | x, y) = \frac{q(C|x)}{q(y|x)}$ if C includes y . As a result, we can see that the contrastive loss for training sample x is proportional to $-\sum_{y \in \mathcal{Y}} \sum_{C: y \in C} \frac{q(C|x)}{q(y|x)} p_{\text{data}}(y | x) \log \frac{\exp(\phi_\theta(x, y))}{\sum_{y' \in C} \exp(\phi_\theta(x, y'))}$, which is equal to $\mathbb{E}_{q(C|x)} \left[-\sum_{y \in C} \frac{p_{\text{data}}(y|x)}{q(y|x)} \log \frac{\exp(\phi_\theta(x, y))}{\sum_{y' \in C} \exp(\phi_\theta(x, y'))} \right] = \mathbb{E}_{q(C|x)} [D_{\text{KL}}(r^C \| p_\theta^C)] + \text{const. w.r.t. } \theta$. Here we use r^C and p_θ^C to refer to the probability distributions $r^C(y | x) = \frac{p_{\text{data}}(y|x)/q(y|x)}{\sum_{y' \in C} p_{\text{data}}(y'|x)/q(y'|x)}$ and $p_\theta^C(y | x) = \frac{\exp(\phi_\theta(x, y))}{\sum_{y' \in C} \exp(\phi_\theta(x, y'))}$, whose supports are $C \subset \mathcal{Y}$. Since we are minimizing the KL divergence under all possible $C \subset \mathcal{Y}$, the global optima will be the ones that make $p_\theta(y | x)$ equal to $r(y | x)$ for all $y \in \mathcal{Y}$ if $\phi_\theta(x, y)$ is expressive enough to fit the target distribution arbitrarily close. Note that $\phi_\theta(x, y)$ is indeed expressive enough since we implement it as a neural network, due to the universal approximation theorem [12, 19]. The two losses hence have the same global optima. \square

Remark 1. The implication of Theorem 1 is that the contrastive loss (Eq. 3) can approximately reduce the exposure bias if we set the proposal distribution $q(y | x)$ to be the propensity score, i.e. the probability that the old systems deliver item y to user x when we were collecting the training data \mathcal{D} .

2.3 Practical Implementations of Contrastive Learning for Large-Scale DCG

We now describe our implementations of the debiased contrastive loss for large-scale DCG.

We first note that the propensity score $q(y | x)$ is not easy to estimate in practice, because industrial recommender systems involve many complicated stages and the data are also highly sparse. Moreover, some theoretical results [34] have pointed out that small propensities can lead to high variance that harms overall performance, and thus the accurate propensity scores may not perform better than the smoothed inaccurate propensities. We thus use $q(y)$ in place of $q(y | x)$, i.e. assuming $q(y | x) \approx q(y)$, to ease estimation and avoid small propensities. Secondly, $q(y)$ (i.e. the probability that item y is recommended to some user) has an extremely high correlation with $p_{\text{data}}(y)$, i.e. the probability that item y is being recommended and clicked by someone, because the existing system will mainly recommend items that have a high click-through rate if it is already highly optimized. We thus further replace $q(y)$ with $p_{\text{data}}(y)$, i.e. assuming $q(y) \approx p_{\text{data}}(y)$, to ease implementation. In summary, we assume $q(y | x) \approx p_{\text{data}}(y)$, which allows us to draw negative samples from \mathcal{D} directly when implementing the contrastive loss for bias reduction. We thus, unlike the IPW methods, do not need to introduce an extra stage into the training pipeline.

However, sampling will still incur non-negligible overheads, e.g. communication costs, in a distributed environment [37], and cannot guarantee that every item will be sampled in an epoch. We thus adopt a queue-based design [16] that avoids explicitly performing sampling, as shown in Figure 1b and Figure 1c. To be specific, we maintain a first-in first-out (FIFO) queue \mathcal{Q} , which has a fixed capacity and can store $|\mathcal{Q}|$ examples. Given a new batch to process, we first enqueue the positive examples y (or their representations $g_\theta(y)$) encountered in the present batch into \mathcal{Q} . We then use the examples stored in the queue as $\{y\} \cup \{y_i\}_{i=1}^L$ (including one positive example and L negative examples) to compute the denominator of the contrastive loss (Eq. 3) for the present batch. In a distributed setting, each worker maintains its own queue locally to avoid communication costs. When the queue size $|\mathcal{Q}|$ is equal to the batch size, our implementation is then equivalent to sampling negative examples from the present batch [35, 17, 10] (see Figure 1a). In general, we need thousands of negative samples to achieve satisfying

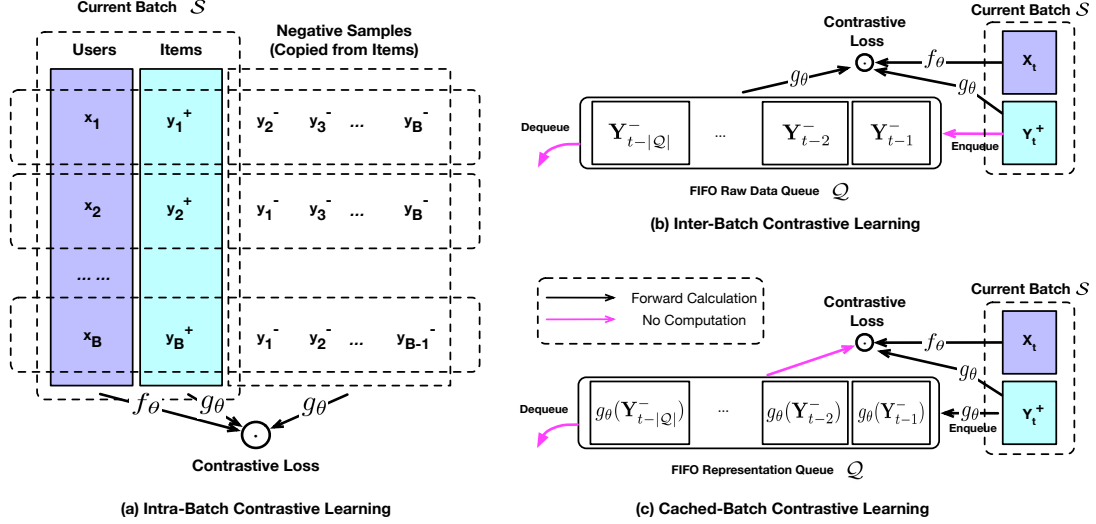


Figure 1: Three implementations of CLRec, whose implicit proposal distributions are $q(y | x) = p_{\text{data}}(y)$. The superscripts $+$, $-$ mean positive and negative examples respectively. Implementation (a) uses the positive examples of other instances in the present batch as the negative examples. Implementation (b) creates a fixed-size FIFO queue to store the positive examples encountered in previously processed batches, and use the examples stored in the queue to serve as the negative examples for the present batch. Implementation (c) differs from implementation (b) in that the queue caches the computed representations $g_{\theta}(y)$ rather than storing the raw features of y .

performance. We therefore use a large queue size, but with a small batch size to prevent out-of-memory, e.g. batch size = 256 and queue size = 2,560.

With the implementation that caches $g_{\theta}(y)$ (see Figure 1c), we can no longer back-propagate through the negative examples from the previous batches, though we can still back-propagate through the negative examples from the present batch. As a result, we find that the total training steps required for convergence mildly increase. However, since each training step will take much less time to compute (and less communication costs in a distributed training setting), the total running time can still be greatly reduced if the features of the negative items are expensive to encode, e.g. if the features contain raw images, texts, or even structured data such as a knowledge graph.

3 Experiment

In this section, we report both offline and online results in a large-scale e-commerce recommender system, as well as offline results on public datasets to ensure reproducibility.

3.1 Online and Offline Experiments in Production Environments

The online experiments have lasted for four months, and our algorithm serves several scenarios with different traffic volumes. We leave some details to the supplemental material, e.g., hyper-parameters and evaluation metrics as well as the features used in Section B, details of the encoders in Section C, and details of the baselines in Section D. The total number of items for recommendation is around 100 million. We use the queue-based implementation without caching in this section, while we will explore settings where encoding is much more expensive and requires caching in Subsection 3.2.

3.1.1 The Debiasing Effect in Large-Scale Production Environments

To examine the debiasing effects of CLRec, we first conduct offline experiments and compare CLRec with sampled softmax. We report the aggregated diversity [2] in Table 1, and the distributions of the recommended items resulted from the different losses in Figure 2.

Table 1 shows that CLRec has an over $2\times$ improvement on aggregated diversity. We see from Figure 2 that, sampled softmax tends to faithfully fit the distribution of the training data. CLRec, however, learns a relatively different distribution, which shifts towards the under-explored items. These results suggest that CLRec does result in a fairer algorithm that alleviates the “rich-get-richer” phenomenon.

This debiasing effect not only leads to a fairer system, but also contributes to a significant improvement regarding the online performance. In Table 2, we compare CLRec with other sampling alternatives using

Table 1: Aggregate diversity [2], i.e. the number of distinct items recommended to a random subset of users.

	Aggregated Diversity
samplerd-softmax	10,780,111
CLRec	21,905,318

Table 2: CLRec vs. the sampling-based alternatives. We conducted these proof-of-concept live experiments in a small-traffic scenario, due to the costs of online experiments. The negative sampling baseline has been outdated and removed from our live system before this work starts.

Method	HR@50	CTR(online)
negative sampling	7.1%	outdated
shared negative sampling	6.4%	-
samplerd-softmax	17.6%	3.32%
CLRec	17.8%	3.85%

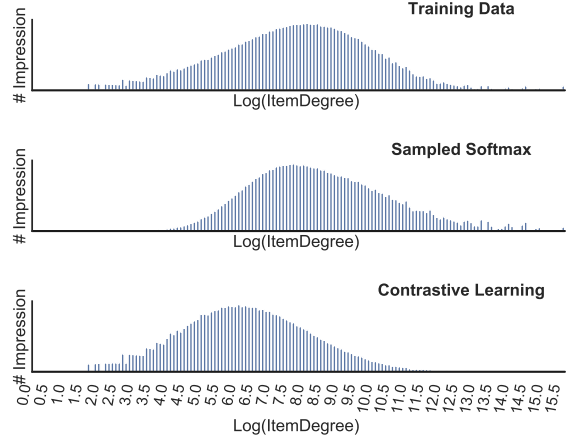


Figure 2: The total number of impressions of the items in a specific degree bucket vs. the logarithm of the corresponding degree. The rightmost bar is not the highest because the number of the extremely popular items is small, even though each item in the bucket has an extremely high degree.

Table 3: Main live experiment results conducted in one of the largest scenarios on our platform. CLRec consistently outperforms the baseline for months and has been fully deployed since Feb 2020.

Method	CTR	Average Dwell Time	Popularity Index of Recommended Items
MIND	5.87%	-	0.658 (high \rightarrow tend to recommend popular items)
CLRec	6.30%	+11.9%	0.224 (low \rightarrow fair to under-explored items)

the same implementation of the encoders. Details of the alternative methods can be found in Section D of the supplemental material. We observe that negative sampling [31], including its variant [46] that makes the instances in a batch share the same large set of negative samples, does not perform well in our settings. CLRec’s improvement over samplerd-softmax [21, 5] w.r.t. the offline metric HitRate@50 is negligible. However, CLRec achieves significant improvement regarding the click-through rate (CTR) online. This indicates that there exists discrepancy between the offline metric and the online performance.

3.1.2 Four Months’ Large-Scale A/B testing

CLRec has been fully depolyed into several heavy-traffic scenarios since Feb 2020, after the initial proof-of-concept ablation studies shown in Table 2. Table 3 shows our main online results conducted in these heavy-traffic scenarios, with billions of page views each day. During the four months’ A/B testing, CLRec has been consistently outperforming MIND [26], the previous state-of-art baseline, in terms of the fairness metrics such as aggregated diversity and average popularity index, as well as the user engagement metrics such as click-through rate and average dwell time ².

Compared with MIND [26], which is the previous state-of-art DCG baseline deployed in the system, CLRec tends to recommend items with a lower popularity index while being more attractive to the users. This proves CLRec’s ability of identifying high-quality items that are rarely explored by the previous systems. We further achieve a +2% relative improvement in the total click number on our platform after ensembling CLRec and MIND, compared to using MIND as the only DCG method.

3.2 Computational Feasibility of CLRec on Complex Pretext Tasks

Efficiency Table 4 compares CLRec and samplerd-softmax in terms of training speed and the network traffic required in a distributed setting. CLRec’s queue-based implementation is much more efficient than the methods that perform explicit sampling, since CLRec reuses the result computed for a positive sample shortly later when the sample is serving as a negative sample. The version of samplerd-softmax

²See Subsection B.2 of the supplemental material for the definitions of the fairness and engagement metrics.

Table 4: Efficiency. We report the training speed in terms of the number of the positive examples processed per second, and the average network traffic of the workers in a distributed environment.

Method	Examples Per Second	Network Traffic (MB/s)
sampled-softmax + negatives w/o features	$\approx 280k$	≈ 700
sampled-softmax + negatives with features	$\approx 130k$	$\approx 1,100$
CLRec + negatives w/o features	$\approx 330k$	≈ 500
CLRec + negatives with features	$\approx 280k$	≈ 500

Table 5: Task u2i is the regular task where x is a sequence of clicks and y is the next click to be predicted. Task u2u adds an auxiliary loss where x and y are both sequences from the same user (before and after a sampled timestamp), which is co-trained with task u2i. Task u2u is a complex pretext task that requires the cached implementation due to high costs when encoding the negative samples. HR1@50 and HR5@50 represent HR@50 for predicting next one and five clicks respectively.

Task & Implementation	HR1@50	HR5@50
CLRec-u2i	17.9%	12.1%
CLRec-u2u, cached	18.3%	12.7%
CLRec-u2u, cached + MoCo	18.2%	12.6%

Table 6: The benefits of encoding features for the negative samples. Most baselines that employ sampled-softmax do not encode rich features for the negative samples (though they still use features when encoding the users’ click sequences), because the number of negative samples is large and brings high costs if the features are complex. Fortunately, CLRec’s cached implementation greatly reduces the costs, as demonstrated in Table 4.

Method	HR@50
CLRec + negatives w/o features	17.4%
CLRec + negatives with features	19.4%

that encodes features for the negative items is from [50]. This proof-of-concept experiment only uses categorical features of the items, and we can deduce that the improvement regarding efficiency will be much more substantial with more complex features. Table 6 shows that encoding features for the negative samples is beneficial, which justifies the efforts spent on efficiency.

Complex Pretext Task that Requires the Cached Implementation We now demonstrate that CLRec with a queue that caches the computed results can enable more complex pretext tasks that may improve the quality of the learned representations. To be more specific, we consider an auxiliary task where x and y are both sequences from the same user (before and after a sampled timestamp). The goal is to identify the correct sequence y that belongs to the same user that produces x . More details can be found in Section E of the supplemental material. This auxiliary task is previously too expensive to implement with sampled-softmax, since the negative samples are sequences and are thus expensive to encode. Fortunately, cached CLRec can implement this task efficiently. Table 5 demonstrates that the auxiliary task can improve an algorithm’s ability to make long-term prediction.

MoCo (short for momentum contrast) [16] proposes a momentum method for updating the encoders based on the cached results and for stabilizing the training loss. We observe no gain with MoCo, possibly because (1) our model is shallow compared to those for visual tasks, and (2) we have a large embedding table which serves as a consistent dictionary that prevents the loss from oscillating.

3.3 Experiments on Public Dataset

To ensure reproducibility, we also conduct experiments on three public datasets from the existing approaches [24, 38]. Our source code will be released. We strictly follow the settings and metrics used by BERT4Rec [38] and report the results in Table 7. Note that the metrics used by BERT4Rec [38] penalizes false positive predictions on popular negative items. As a result, CLRec achieves a significant performance gain thanks to bias reduction. Qualitative results that illustrate the debiasing effects, similar to those in Subsection 3.1.1, can be found in Section F of the supplementary material.

4 Related Work

Deep Candidate Generation Deep candidate generation methods are widely deployed in industrial systems, e.g., YouTube [11, 22, 9], Taobao [48, 26, 29, 49], and Pinterest [46]. The existing methods explicitly sample negative examples from a pre-defined proposal distribution [31, 21, 5]. The proposal distribution not only affects convergence, but also has a significant impact on the performance [8].

Table 7: Results on public benchmarks to ensure reproducibility. For fair comparison, the CLRec implementation here uses the same Transformer [28] encoder as SASRec but with a contrastive loss.

Method	Metric	ML-1M	Beauty	Steam	Metric	ML-1M	Beauty	Steam
SASRec	HR@1	0.2351	0.0906	0.0885	NDCG@5	0.3980	0.1436	0.1727
BERT4Rec		0.2863	0.0953	0.0957		0.4454	0.1599	0.1842
CLRec		0.3013	0.1147	0.1325		0.4616	0.1876	0.2396
Improv.		+5.2%	+20.4%	+38.4%		+3.6%	+17.3%	+30.0%
SASRec	HR@5	0.5434	0.1934	0.2559	NDCG@10	0.4368	0.1633	0.2147
BERT4Rec		0.5876	0.2207	0.2710		0.4818	0.1862	0.2261
CLRec		0.6045	0.2552	0.3413		0.4988	0.2156	0.2852
Improv.		+2.9%	+15.6%	+25.9%		+3.5%	+15.8%	+26.1%
SASRec	HR@10	0.6629	0.2653	0.3783	MRR@1	0.3790	0.1536	0.1874
BERT4Rec		0.6970	0.3025	0.4013		0.4254	0.1701	0.1949
CLRec		0.7194	0.3423	0.4829		0.4417	0.1968	0.2457
Improv.		+3.2%	+13.1%	+20.3%		+3.8%	+15.7%	+26.0%

Empirically the number of the negative samples need to be large, e.g. a few thousand ones for pairing with a positive example. Consequently, it is computationally expensive to incorporate rich features for the negative samples. The existing systems hence usually choose to not encode features for the negative examples except for simple features such as item IDs [11], even though rich features for the negative samples are demonstrated to be beneficial [4]. CLRec achieves great efficiency when encoding rich features for the negative samples by caching the computed results.

Bias Reduction and Fairness in Recommender Systems Recommendation algorithms that directly fits the training data will suffer from selection bias due to the missing-not-at-random phenomenon [34], where the previous recommendation algorithms affect the training data collected. The topic of reducing the bias in training and evaluating recommender systems has been explored before [36, 3, 43, 34, 9, 45]. However, these existing works mostly focus on small-scale offline settings, and rely on techniques impractical for large-scale DCG. For example, most of them involve an extra stage to train a propensity score estimator. We also find that dividing the propensity scores leads to numerical instability and thus fail to achieve satisfying results. Correcting the bias helps improve P-fairness [7], i.e. fairness towards the previously under-recommended products [6].

Contrastive Learning Contrastive learning, which aims to learn high-quality representations via self-supervised pretext tasks, recently achieves remarkable successes in various domains, e.g., speech processing [32], computer vision [18, 16], graph data [41], and compositional environments [25]. The contrastive loss we investigate in this paper is a generalization of the InfoNCE loss [32]. InfoNCE is previously understood as a bound of the mutual information between two variables [32]. Our work provides a new perspective on the effectiveness of the contrastive loss, by illustrating its connection with inverse propensity weighting [33, 20, 39], a well-known technique for bias reduction.

5 Conclusion

We established in theory the connection between contrastive learning and bias reduction. We then proposed CLRec, a contrastive learning framework for debiased candidate generation, which may lead to a fairer system and can achieve high efficiency when encoding features of complex data types.

Broader Impact

Positive Impact The debiasing effect of our proposed framework CLRec helps to address the producer fairness (i.e. P-fairness) problem [7] in recommender systems, so that high quality items that are previously under-explored get more chances of being presented to the users. It leads to a fairer eco-system. While this paper takes a live e-commerce recommender system as an example to illustrate the benefits of CLRec, we would like to highlight that CLRec can be applied to other domains such as search engines, advertising, the retrieval phase in open domain question answering, as well as other types of recommender systems. Applying CLRec to the various domains may bring:

- Fairer traffic assignment in user-generated content (UGC) platforms.
- Increased diversity of the information being spread in a society by distributing the voices from the minority groups in a fairer manner.
- Fairer opportunities in the job market.

Although there are other studies, e.g. IPW-based approaches, that also aim to reduce data bias, they usually suffer from implementation difficulties and numerical instability during optimization. Moreover, few has targeted specifically at the candidate generation stage in modern recommender systems. We also find little public information on how a debiased method will eventually affect a live system. This paper shares the online experiment results lasted for at least four months and reports positive results, which could be valuable to the community.

Negative Impact A more accurate recommender system means that a user will more easily absorb passively the information that the system presents and the user may become over-reliant on the system. Platforms that provide accurate recommendation service may thus have the power to control what they want their users to see. This a general problem for recommender systems. On the other hand, CLRec prefers under-explored items that have a high potential, and it is not clear whether CLRec will be more prone to adversarial attacks.

References

- [1] M. Abadi, P. Barham, J. Chen, Z. Chen, A. Davis, J. Dean, M. Devin, S. Ghemawat, G. Irving, M. Isard, et al. Tensorflow: A system for large-scale machine learning. In *12th {USENIX} Symposium on Operating Systems Design and Implementation ({OSDI} 16)*, pages 265–283, 2016.
- [2] G. Adomavicius and Y. Kwon. Improving aggregate recommendation diversity using ranking-based techniques. *IEEE Transactions on Knowledge and Data Engineering*, 24(5):896–911, 2011.
- [3] Q. Ai, K. Bi, C. Luo, J. Guo, and W. B. Croft. Unbiased learning to rank with unbiased propensity estimation. In *The 41st International ACM SIGIR Conference on Research & Development in Information Retrieval*, pages 385–394, 2018.
- [4] J. Bai, C. Zhou, J. Song, X. Qu, W. An, Z. Li, and J. Gao. Personalized bundle list recommendation. In *The World Wide Web Conference*, pages 60–71, 2019.
- [5] Y. Bengio and J.-S. Senécal. Adaptive importance sampling to accelerate training of a neural probabilistic language model. *IEEE Transactions on Neural Networks*, 19(4):713–722, 2008.
- [6] A. Beutel, J. Chen, T. Doshi, H. Qian, L. Wei, Y. Wu, L. Heldt, Z. Zhao, L. Hong, E. H. Chi, and C. Goodrow. Fairness in recommendation ranking through pairwise comparisons. In *KDD*, 2019.
- [7] R. Burke. Multisided fairness for recommendation, 2017.
- [8] H. Caselles-Dupré, F. Lesaint, and J. Royo-Letelier. Word2vec applied to recommendation: Hyper-parameters matter. In *Proceedings of the 12th ACM Conference on Recommender Systems*, pages 352–356. ACM, 2018.
- [9] M. Chen, A. Beutel, P. Covington, S. Jain, F. Belletti, and E. H. Chi. Top-k off-policy correction for a reinforce recommender system. In *Proceedings of the Twelfth ACM International Conference on Web Search and Data Mining*, pages 456–464, 2019.
- [10] T. Chen, Y. Sun, Y. Shi, and L. Hong. On sampling strategies for neural network-based collaborative filtering. In *Proceedings of the 23rd ACM SIGKDD International Conference on Knowledge Discovery and Data Mining*, pages 767–776. ACM, 2017.
- [11] P. Covington, J. Adams, and E. Sargin. Deep neural networks for youtube recommendations. In *Proceedings of the 10th ACM Conference on Recommender Systems*, pages 191–198. ACM, 2016.
- [12] G. Cybenko. Approximation by superpositions of a sigmoidal function. *Mathematics of Control, Signals and Systems*, 1989.

- [13] X. Glorot and Y. Bengio. Understanding the difficulty of training deep feedforward neural networks. In *Proceedings of the thirteenth international conference on artificial intelligence and statistics*, pages 249–256, 2010.
- [14] M. Grbovic and H. Cheng. Real-time personalization using embeddings for search ranking at airbnb. In *Proceedings of the 24th ACM SIGKDD International Conference on Knowledge Discovery & Data Mining*, pages 311–320. ACM, 2018.
- [15] M. Gutmann and A. Hyvärinen. Noise-contrastive estimation: A new estimation principle for unnormalized statistical models. In *Proceedings of the Thirteenth International Conference on Artificial Intelligence and Statistics*, pages 297–304, 2010.
- [16] K. He, H. Fan, Y. Wu, S. Xie, and R. Girshick. Momentum contrast for unsupervised visual representation learning. *arXiv preprint arXiv:1911.05722*, 2019.
- [17] B. Hidasi, A. Karatzoglou, L. Baltrunas, and D. Tikk. Session-based recommendations with recurrent neural networks. *arXiv preprint arXiv:1511.06939*, 2015.
- [18] R. D. Hjelm, A. Fedorov, S. Lavoie-Marchildon, K. Grewal, P. Bachman, A. Trischler, and Y. Bengio. Learning deep representations by mutual information estimation and maximization. *arXiv preprint arXiv:1808.06670*, 2018.
- [19] K. Hornik. Approximation capabilities of multilayer feedforward networks. *Neural Networks*, 1991.
- [20] G. W. Imbens and D. B. Rubin. *Causal inference in statistics, social, and biomedical sciences*. Cambridge University Press, 2015.
- [21] S. Jean, K. Cho, R. Memisevic, and Y. Bengio. On using very large target vocabulary for neural machine translation. *arXiv preprint arXiv:1412.2007*, 2014.
- [22] M. R. Joglekar, C. Li, J. K. Adams, P. Khaitan, and Q. V. Le. Neural input search for large scale recommendation models. *arXiv preprint arXiv:1907.04471*, 2019.
- [23] J. Johnson, M. Douze, and H. Jégou. Billion-scale similarity search with gpus. *arXiv preprint arXiv:1702.08734*, 2017.
- [24] W.-C. Kang and J. McAuley. Self-attentive sequential recommendation. In *2018 IEEE International Conference on Data Mining (ICDM)*, pages 197–206. IEEE, 2018.
- [25] T. Kipf, E. van der Pol, and M. Welling. Contrastive learning of structured world models. *arXiv preprint arXiv:1911.12247*, 2019.
- [26] C. Li, Z. Liu, M. Wu, Y. Xu, H. Zhao, P. Huang, G. Kang, Q. Chen, W. Li, and D. L. Lee. Multi-interest network with dynamic routing for recommendation at tmall. In *Proceedings of the 28th ACM International Conference on Information and Knowledge Management*, pages 2615–2623, 2019.
- [27] D. Liang, R. G. Krishnan, M. D. Hoffman, and T. Jebara. Variational autoencoders for collaborative filtering. In *Proceedings of the 2018 World Wide Web Conference, WWW '18*, pages 689–698, 2018.
- [28] Z. Lin, M. Feng, C. N. d. Santos, M. Yu, B. Xiang, B. Zhou, and Y. Bengio. A structured self-attentive sentence embedding. *arXiv preprint arXiv:1703.03130*, 2017.
- [29] J. Ma, C. Zhou, P. Cui, H. Yang, and W. Zhu. Learning disentangled representations for recommendation. In *Advances in Neural Information Processing Systems*, pages 5712–5723, 2019.
- [30] A. McCallum, K. Nigam, et al. A comparison of event models for naive bayes text classification. In *AAAI-98 workshop on learning for text categorization*, pages 41–48. Citeseer, 1998.
- [31] T. Mikolov, I. Sutskever, K. Chen, G. S. Corrado, and J. Dean. Distributed representations of words and phrases and their compositionality. In *Advances in neural information processing systems*, pages 3111–3119, 2013.
- [32] A. v. d. Oord, Y. Li, and O. Vinyals. Representation learning with contrastive predictive coding. *arXiv preprint arXiv:1807.03748*, 2018.

- [33] P. R. Rosenbaum and D. B. Rubin. The central role of the propensity score in observational studies for causal effects. *Biometrika*, 70(1):41–55, 1983.
- [34] T. Schnabel, A. Swaminathan, A. Singh, N. Chandak, and T. Joachims. Recommendations as treatments: Debiasing learning and evaluation. *arXiv preprint arXiv:1602.05352*, 2016.
- [35] K. Sohn. Improved deep metric learning with multi-class n-pair loss objective. In *Advances in Neural Information Processing Systems*, pages 1857–1865, 2016.
- [36] H. Steck. Evaluation of recommendations: rating-prediction and ranking. In *Proceedings of the 7th ACM conference on Recommender systems*, pages 213–220, 2013.
- [37] S. Stergiou, Z. Straznickas, R. Wu, and K. Tsioutsoulouklis. Distributed negative sampling for word embeddings. In *Thirty-First AAAI Conference on Artificial Intelligence*, 2017.
- [38] F. Sun, J. Liu, J. Wu, C. Pei, X. Lin, W. Ou, and P. Jiang. Bert4rec: Sequential recommendation with bidirectional encoder representations from transformer. In *Proceedings of the 28th ACM International Conference on Information and Knowledge Management*, pages 1441–1450, 2019.
- [39] S. K. Thompson. *Sampling*. Wiley, 2012.
- [40] A. Vaswani, N. Shazeer, N. Parmar, J. Uszkoreit, L. Jones, A. N. Gomez, L. Kaiser, and I. Polosukhin. Attention is all you need. *arXiv preprint arXiv:1706.03762*, 2017.
- [41] P. Veličković, W. Fedus, W. L. Hamilton, P. Liò, Y. Bengio, and R. D. Hjelm. Deep graph infomax. *arXiv preprint arXiv:1809.10341*, 2018.
- [42] H. Wang, Y. Wang, Z. Zhou, X. Ji, D. Gong, J. Zhou, Z. Li, and W. Liu. Cosface: Large margin cosine loss for deep face recognition. In *Proceedings of the IEEE Conference on Computer Vision and Pattern Recognition*, pages 5265–5274, 2018.
- [43] X. Wang, M. Bendersky, D. Metzler, and M. Najork. Learning to rank with selection bias in personal search. In *Proceedings of the 39th International ACM SIGIR conference on Research and Development in Information Retrieval*, pages 115–124, 2016.
- [44] N. Wojke and A. Bewley. Deep cosine metric learning for person re-identification. In *2018 IEEE winter conference on applications of computer vision (WACV)*, pages 748–756. IEEE, 2018.
- [45] L. Yang, Y. Cui, Y. Xuan, C. Wang, S. Belongie, and D. Estrin. Unbiased offline recommender evaluation for missing-not-at-random implicit feedback. In *Proceedings of the 12th ACM Conference on Recommender Systems*, pages 279–287, 2018.
- [46] R. Ying, R. He, K. Chen, P. Eksombatchai, W. L. Hamilton, and J. Leskovec. Graph convolutional neural networks for web-scale recommender systems. *arXiv preprint arXiv:1806.01973*, 2018.
- [47] C. Zhou, J. Bai, J. Song, X. Liu, Z. Zhao, X. Chen, and J. Gao. Atrank: An attention-based user behavior modeling framework for recommendation. In *Thirty-Second AAAI Conference on Artificial Intelligence*, 2018.
- [48] C. Zhou, Y. Liu, X. Liu, Z. Liu, and J. Gao. Scalable graph embedding for asymmetric proximity. In *Thirty-First AAAI Conference on Artificial Intelligence*, 2017.
- [49] H. Zhu, X. Li, P. Zhang, G. Li, J. He, H. Li, and K. Gai. Learning tree-based deep model for recommender systems. In *Proceedings of the 24th ACM SIGKDD International Conference on Knowledge Discovery & Data Mining*, pages 1079–1088. ACM, 2018.
- [50] R. Zhu, K. Zhao, H. Yang, W. Lin, C. Zhou, B. Ai, Y. Li, and J. Zhou. Aligraph: a comprehensive graph neural network platform. *Proceedings of the VLDB Endowment*, 12(12):2094–2105, 2019.

A Inverse Propensity Weighting for Debiased Candidate Generation

In this section, we assume that the recommender system is a sequential recommender system where a user will receive only one recommendation y when the user's state becomes x . However, we note that it is easy to verify that our conclusions still hold when user state x receives K recommendations, where $K \geq 1$. We will also focus on a single user state x for conciseness.

A.1 Training with Unbiased Data

Ideally, we should collect the training data that do not suffer from selection bias. This is equivalent to collect training data under a random recommendation policy π_{uni} that always recommends a random item in a uniform way, i.e., the random policy should not be aware of the value of x and y .

Let the oracle user preference be $p(\text{click} = 1 | x, y)$, which is a bernoulli distribution and represents how likely user x will click item y if we recommend item y to the user. Assuming that user x clicks one item recommended by the random policy π_{uni} , the click data collected under π_{uni} will be:

$$p_{\pi_{\text{uni}}}(y|x) = \frac{p(\text{click} = 1 | x, y)}{\sum_{y'} p(\text{click} = 1 | x, y')}, \quad (5)$$

which is the oracle click data distribution for unbiased training, since the uniform random policy π_{uni} does not introduce any selection bias. Note that $p_{\pi_{\text{uni}}}(y|x)$ is a multinomial distribution rather than a multivariate bernoulli distribution.

To learn an unbiased recommendation policy, we need to optimize $p_{\theta}(y|x)$ on the click data collected under the uniform random policy. In other words, the unbiased loss function should be:

$$R(\theta|x) = - \sum_y p_{\pi_{\text{uni}}}(y|x) \log p_{\theta}(y|x). \quad (6)$$

A.2 Training with Biased Data: Inverse Propensity Weighting

However, random exploration is expensive in a real-world recommender system. In practice, the click data \mathcal{D}_{π} for training a new policy is collected under a biased old recommendation policy π . Let $q_{\pi}(y | x)$ be the probability that the old policy recommends item y to a user in state x . Note that $q_{\pi}(y | x)$ is a multinomial distribution, i.e. $\sum_{y'} q_{\pi}(y' | x) = 1$.

The generating process of the biased dataset \mathcal{D}_{π} is as follows. Policy π makes a recommendation, i.e. draws a one-hot impression vector O from the multinomial distribution $q_{\pi}(y | x)$, whose y th element $O_y = 1$ if the recommendation is item y , and $O_y = 0$ otherwise. On the other hand, user x is associated with a multi-hot vector C representing the user's preference regarding all the items, whose y th element C_y is drawn from the bernoulli distribution $p(\text{click} = 1 | x, y)$, $y = 1, 2, 3, \dots, |\mathcal{Y}|$. Here $C_y = 1$ if the user will click item y after being recommended item y , $C_y = 0$ otherwise.

A naïve estimator that does not take selection bias into account typically learns a new biased policy $p_{\theta}(y|x)$ by minimizing the following biased loss:

$$\hat{R}_{\text{naive}}(\theta|\mathcal{D}_{\pi}) = - \sum_y O_y C_y \log p_{\theta}(y|x), \quad (7)$$

Since O and C are independent, the expectation of the above loss is

$$\mathbb{E}_{\mathcal{D}_{\pi}} [\hat{R}_{\text{naive}}(\theta|\mathcal{D}_{\pi})] = - \sum_y \mathbb{E}[O_y] \mathbb{E}[C_y] \log p_{\theta}(y | x) \quad (8)$$

$$= - \sum_y q_{\pi}(y | x) p(\text{click} = 1 | x, y) \log p_{\theta}(y | x). \quad (9)$$

The naïve estimator is thus not optimizing the ideal loss as described in Eq. (6).

Now let us analyze the IPW estimator, which minimizes the following loss:

$$\hat{R}_{\text{IPW}}(\theta|\mathcal{D}_{\pi}) = - \sum_y \frac{1}{q(y | x)} O_y C_y \log p_{\theta}(y | x). \quad (10)$$

Note that $p_{\pi_{\text{uni}}}(y|x) \propto p(\text{click} = 1 \mid x, y)$ according to Eq. (5). We thus have:

$$\mathbb{E}_{\mathcal{D}_{\pi}} \left[\hat{R}_{\text{IPW}}(\theta | \mathcal{D}_{\pi}) \right] = - \sum_y \frac{q_{\pi}(y \mid x)}{q(y \mid x)} p(\text{click} = 1 \mid x, y) \log p_{\theta}(y \mid x) \quad (11)$$

$$\propto - \sum_y \frac{q_{\pi}(y \mid x)}{q(y \mid x)} p_{\pi_{\text{uni}}}(y \mid x) \log p_{\theta}(y \mid x). \quad (12)$$

We can see that, if we set $q(y|x)$ to $q_{\pi}(y|x)$, the IPW estimator is then an unbiased estimation that minimizes the oracle unbiased loss Eq. (6).

A.3 Bernoulli Propensities vs. Multinomial Propensities

We note that our fomulation is different from the existing literature on debiasing a recommender [36, 3, 43, 34, 9, 45]. Most of the existing methods assume that the recommendations O are drawn from a multivariate bernoulli policy, i.e., O_y follows an independent bernoulli distribution $q_{\pi}(\text{recommend} = 1 \mid x, y)$ [43, 34]. Here $O_y \in \{0, 1\}$ denotes whether item y is recommended by the policy. We take a different approach and instead assume that O is drawn from a multinomial policy $q_{\pi}(y \mid x)$ rather than a multivariate bernoulli one.

In other words, the difference lies in whether we should design a candidate generation policy as a multinomial model or as a multivariate bernoulli model. We choose to design the policy as a multinomial one, due to the following reasons:

- *The multinomial formulation brings superior performance.* There are many empirical results that report better performance with a multinomial candidate generation method than a multivariate bernoulli one, especially with a large set of items for recommendation [11, 26, 21, 27]. Our empirical results in Table 2, where the negative sampling baselines follow the multivariate bernoulli formulation, also verify this finding. Similarly, the natural language processing (NLP) community also report better results with a multinomial classifier, especially when the number of classes increases [30].
- *The multinomial formulation is more consistent with the real-world production environments.* The multivariate bernoulli formulation implicitly assumes that the number of recommendations requested by a user can be modeled as part of the recommendation policy π , e.g., the expectation of the number of recommendations is $\sum_y q_{\pi}(\text{recommend} = 1 \mid x, y)$ with the multivariate bernoulli formulation. However, this assumption does not hold in many recommender systems, where the number of recommendations received by a user is decided by the user rather than the system. For example, the user can request more recommendations by scrolling down the page or stop receiving any new recommendation by leaving the page. On the contrary, the multinomial policy $q_{\pi}(y \mid x)$ does not attempt to model the number of recommendations requested by a user. Rather, the multinomial policy $q_{\pi}(y \mid x)$ only models which one item it should recommend if the user explicitly requests the system to make one recommendation.

B Experimental Settings

B.1 Public Datasets

Statistics of the public datasets can be found in Table 8. We follow the baselines’ setting [38] and construct the test set by pairing the ground-truth positive clicks with the negative items sampled according to their popularity. We find that this way of constructing the test set shares similar spirits with the less biased evaluator [45] which uses the IPW technique to emphasize the importance of making correct predictions for the less popular items.

B.2 Production Environments

Data and Hyper-parameters We use the data collected from the last four days on our platform as the training data and use the click data recorded in the following day as the test set. We limit

¹<http://jmcauley.ucsd.edu/data/amazon/>

²<https://grouplens.org/datasets/movielens/1m/>

³https://cseweb.ucsd.edu/~jmcauley/datasets.html#steam_data

Table 8: Public dataset statistics.

Dataset	#Users	#Items	#Interactions	Density
Beauty ¹	40,226	54,542	0.35M	0.02%
ML-1M ²	6040	3416	1.0M	4.79%
Steam ³	281,428	13,044	3.5M	0.10%

the minimum length of a valid sequence to be five in the training set, because requiring the model to predict the next item of an unusually short sequence can easily introduce great noise which harms the recommendation performance. We use seven categorical features of the items, including item ID, coarse-grained and fine-grained category IDs, seller ID, seller category, brand ID, and gender preference, for our live experiments. We use the queue-based implementation without the caching mechanism on the regular tasks where the negative items consist of the seven categorical features, while using the queue-based implementation that caches the processed results when solving the complex pretext tasks due to the high costs of encoding the complex negative examples. The queue size is 2,560 while the batch size is 256. We train the model for one epoch in total.

Training Environment The training data contain four billion sequences of user behaviors. We train the model in a distributed TensorFlow cluster that consists of 140 workers and 10 parameter servers. Each worker is equipped with a GPU, which is either GTX 1080 Ti or Tesla P100. Each parameter server is allocated 32GB memory while each worker has 16G memory. Training CLRec on our internal four-day data for one epoch costs less than eight hours for task u2i without caching and less than twelve hours for task u2u with caching.

Online Serving We pre-compute offline the item representations via the item encoder. We then store and index the item representations using an online vector-based kNN service for fast retrieval of top relevant items at serving time. At serving time, our user encoder will infer a user representation $f_\theta(x)$ as the request made by user x arrives and pass the user embedding to the kNN service to find a few hundred relevant items S . The latency for dealing with the query is around 10 ms. The set of relevant items S is then send to be scored by a separate deep ranking model that costs much more computational power and is responsible for constructing the final recommendation list by selecting several top relevant items from S .

Evaluation Metrics We report the performance in terms of the following offline and online metrics:

- HitRate50 (HR50) is an offline metric. We sample a subset of users and compute the metric based on the users’ click sequences to measure an algorithm’s offline performance. We pick the latest one clicks of the users as the label y to predict, and use the users’ sequence prior to y to serve as the input x . We run the algorithm under evaluation to retrieve the top 50 items for each user via kNN searching. If the ground-truth next one click y is in the retrieved 50 items, the algorithm receives a score 1 for this user, or score 0 otherwise. The HitRate@50 of the algorithm is then the average score received by the algorithm.
- The click-through rate (CTR) of an algorithm is the percentage of recommendations made by the algorithm that are finally clicked by the users.
- The average dwell time is the total time spent by the users on reading the details of the items clicked by them, divided by the total number of clicks on our platform.
- The aggregate diversity [2], measured on a sampled subset of users for testing, is the number of distinct items recommended to the subset of users.
- The popularity index of the items recommended by a candidate generation algorithm A is defined as $\frac{\mathbb{E}_A[p_{\text{data}}(y)]}{\max_{A'} \mathbb{E}_{A'}[p_{\text{data}}(y)]}$. Here $p_{\text{data}}(y)$ is the number of times our system recommends item y to the users in the past few weeks before we deploy CLRec into the system, and $\mathbb{E}_A[p_{\text{data}}(y)] = \sum_{y \in \mathcal{Y}} p_{\text{data}}(y) \cdot p(\text{algorithm } A \text{ recommends item } y)$ measures how much an algorithm prefers recommending the items that are already popular. The algorithm A' that has the largest value of $\mathbb{E}_{A'}[p_{\text{data}}(y)]$ in our system is a simple candidate generation method that does not learn vector

Table 9: Effects of the forward positional embedding, backward positional embedding, and time bucket embedding. We conducted these ablation studies about the encoders in a small-traffic scenario.

Method	HR@50 (Offline)	CTR (Online)
ForwardPositionEmbedding	18.5%	-
BackwardPositionEmbedding	18.2%	2.98%
TimeBucketEmbedding	18.9%	-
ForwardPositionEmbedding + TimeBucketEmbedding	16.4%	-
BackwardPositionEmbedding + TimeBucketEmbedding	19.1%	3.25%

Table 10: Performance of the different head aggregation strategies used by the sequence encoder.

Method	HR@50 (Offline)	CTR (Online)
mean pooling	15.1%	3.10%
mean pooling + cosine	18.1%	-
mean pooling + MLP	10.5%	-
mean pooling + MLP + cosine	17.7%	-
concatenation + MLP	17.8%	3.15%
WHA + cosine	19.7%	3.21%

representations, which is used as a fallback to handle the cases when the deep candidate generation methods, i.e. MIND and CLRec, fail to return the results within a time limit.

C Implementation of the Encoders

We describe in this section the implementation details of our encoders for large-scale experiments.

C.1 Item representations

An item’s vector representation is the sum of several parts, i.e. a base item embedding corresponding to its ID number, the concatenation of the item features’ embeddings, a time bucket embedding, as well as a backward positional embedding. The time bucket embedding and the positional embedding are only added when the item representation is to be used by the user encoder $f_{\theta}(x)$ for encoding a historical behavior made by the user x . The output of the item encoder $g_{\theta}(y)$ for item y is the sum of only the base item embedding and the item features’ embeddings.

Time Bucket Embedding The timestamps of the user behaviors are critical for the performance of online recommendation systems. To encode time intervals between consecutive behaviors, we use the embeddings of bucketized time intervals, which is used by previous work [47]. To be specific, given the current timestamp t when the user query arrives and the timestamp b when a behavior was recorded, the time interval $t - b$ is discretized and put into a bucket that corresponds to a specific range. Each bucket has its own vector representation, i.e. bucket embedding.

Reverse Positional Embedding We also find that the positional embedding has extra positive impacts even when the time bucket embedding is already in use. There are two ways to add positional embeddings. The forward way is to view the latest click as if it is at the origin position, i.e. position zero, where the earliest click of a user would then be at different positions depending on the user’s sequence length. The backward way is, on the other hand, to view the earliest click as if it is at position zero, and the latest click would then be at a varying position when the sequence length varies. We surprisingly find that the backward version of the positional embedding brings extra improvement even after the bucket embedding is used, while the forward positional embedding does not. We suspect that the time bucket embedding has already highlighted the recent behaviors, and the backward positional embedding can then behave like the backward direction in a bi-directional LSTM for capturing long-range dependencies.

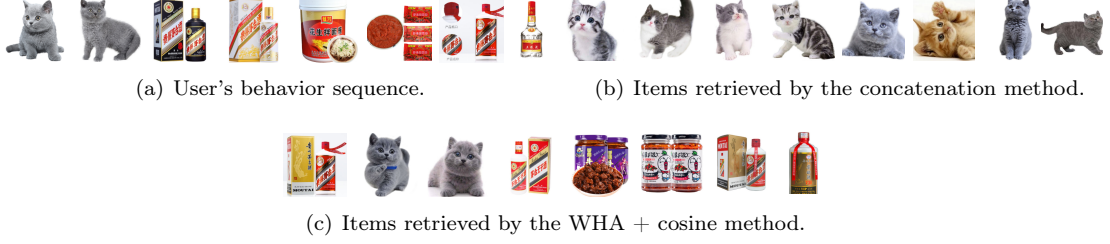


Figure 3: The diversified results with the weighted head aggregation (WHA) layer.

Feature Embedding We encode the categorical and continuous features of an item in a way similar to the previous work [11]. To be specific, we concatenate the features' vector representations and multiple the concatenated result by a linear projection matrix before adding it onto the base embedding.

C.2 User Representations

In a comprehensive e-commerce platform, a user usually has diversified interests that meet various daily demands, leading to a behavior sequence containing multiple interests. We employ a simplified multi-head attention (MultAttn) module, which captures the user's different interests revealed by the input sequence $x = \{y_t\}_{t=1}^T$, as the basis of our user encoder. We then use a module that performs weighted head aggregation (WHA) on top of the representations of the multiple heads. That is:

$$f_{\theta}(x) = \text{WHA}(\text{MultAttn}(\{e_t\}_{t=1}^T)),$$

where $\{e_t\}_{t=1}^T$ are the item representations of the clicks $\{y_t\}_{t=1}^T$ described in the previous subsection.

Next we will introduce the design choice of each part.

Multi-Head Attention Multi-head self-attention [40] achieves great successes in various NLP tasks and is adopted by sequential recommendation models [24, 47]. It is more engineering-efficient than RNN and has superior power to capture multiple semantics of the behaviors with a certain degree of interpretability. Here we simplify self-attention [28] and implement the following module:

$$\text{MultAttn}(X) = \text{softmax}(\text{FFN}(X)^T)X,$$

where $X^{T \times D}$ is the input embedding, FFN is a two-layer feed forward neural network whose output is the attention score $\in \mathbb{R}^{H \times T}$. Here D, T, H are the number of representation dimensions, the length of the sequence, and the number of heads, respectively.

Weighted Heads Aggregation After the simplified multi-head attention module, there are H head representations $\{h_k\}_{k=1}^H$. We use a WHA module to aggregate the heads into one single vector. WHA first computes a global feature vector of m , based on which another weighted attention is performed to produce the final representation e_x of user x :

$$m = \frac{1}{H} \sum_{k=1}^H h_k, \quad d_k = h_k^T M m, \quad a_k = \frac{\exp(d_k)}{\sum_{k'=1}^H \exp(d_{k'})}, \quad e_x = \sum_{k=1}^H a_k h_k, \quad (13)$$

where $M \in \mathbb{R}^{D \times D}$ is a learnable parameter. We find WHA to be more effective than other alternatives such as mean-pooling and concatenation.

We note that, however, WHA seems to be sensitive to the similarity metrics used. In particular, we find that we have to l_2 -normalize the head embeddings before sending them into the WHA module, which improves convergence and helps improve the diversity of the items retrieved. We also choose to normalize the vector output by WHA. Some efforts [42, 44, 29] have been spent on analyzing the cosine similarity related with normalization as well as the positive effects brought by normalization. According to [44], if $p(x|y)$ follows Gaussian distribution, cosine softmax will force the embeddings to form more compact clusters, which makes kNN search more easy. The embeddings should use normal initialization [13] instead of uniform initialization if normalization is in use, so that the initial embeddings can be uniformly

Table 11: Aggregate diversity on public benchmarks, when the candidate generation algorithms with different loss functions are requested to retrieve top ten items for each test user.

Dataset	#Users	Aggregate Diversity		
		Oracle Next Clicks	Sample-Softmax	Contrastive Learning
ML-1M	6,040	1,883	2,348	3,020
Beauty	40,226	19,820	24,340	44,408
Steam	281,428	10,006	5,154	10,111

spread over the hyper-spherical surface, which can prevent the loss from oscillating at the beginning of the training procedure.

In our live experiment, we also find WHA to be critical for our encoders to produce diversified recommendation lists that reflects the different intents behind a user’s behavior sequence. Without WHA, we observe that the retrieved item set can be easily dominated by one single intent, showing limited diversity (see Figure 3).

C.3 Similarity Score Function

We use the cosine similarity with temperature $\tau > 0$ as the similarity function, i.e. $\phi_\theta(x, y) = \frac{\langle f_\theta(x), g_\theta(y) \rangle}{\tau}$ assuming that $f_\theta(x)$ and $g_\theta(y)$ are both l_2 -normalized. We set $\tau = 0.07$ following previous work [16]. We use normalization to stabilize contrastive learning.

C.4 Ablation Study of the Encoders’ Design

We note that each of the following experiments should be taken as the analysis for each component individually, which are conducted during different time periods. Note that, considering the costs of deployment into a live system, we deploy a model online only if it has at least similar performance with the previous baselines. We do not deploy a method online if it has poor performance offline. We mark a method’s online performance as “-” in the table if it is not deployed.

We illustrate in Table 9 and Table 10 that the encoders can benefit from the combination of WHA and cosine similarity and the combination of time bucket embedding and backward positional embedding, respectively. As can be seen in Table 10, cosine similarity is needed to reach a higher HitRate for our production system.

We find that the previous methods, especially those use dot product instead of cosine similarity, easily lead to a much skewer interest distribution of the top-k retrieved items. These previous methods tend to under-explore items from the less popular interests. Many have also noticed this issue and proposed their solutions, such as using multiple interest vectors [29, 26] or multiple interest sub-models [49]. To further verify our conjecture, we conduct case studies in Figure 3 on the retrieved items from different designs of the encoders. We can see that, given the diversified interests in the user’s behavior sequence, which includes spirit, cat and condiment, the encoders without the WHA layer retrieves cats only, while the results of the encoders with WHA and cosine similarity preserve all the interests.

D Implementations of Loss Functions and Sampling Strategies

We list here the details of the loss functions and sampling strategies being compared in Table 2:

- Negative sampling [31]: We sample L examples to pair with each positive click from a proposal distribution $q(y)$. The proposal distribution $q(y)$ is proportional to the item’s degree, i.e., $\text{degree}(y)^{0.75}$ as recommended in [31]. We use a distributed version of the sampling strategy based on the alias method [37], which is provided by the open-source package AliGraph [50]. We tune L ranging from 8 to 2,560 and report the best results.
- Shared negative sampling [46]: This variant of negative sampling aims to increase the efficiency of the original implementation of negative sampling. It makes the positive examples in the present batch share the same set of L negative samples, rather than sampling a different set of L negative samples for each positive instance. Note that sampled softmax, as well as CLRec, similarly let the positive examples in a batch share the same set of negative samples. However, this implementation

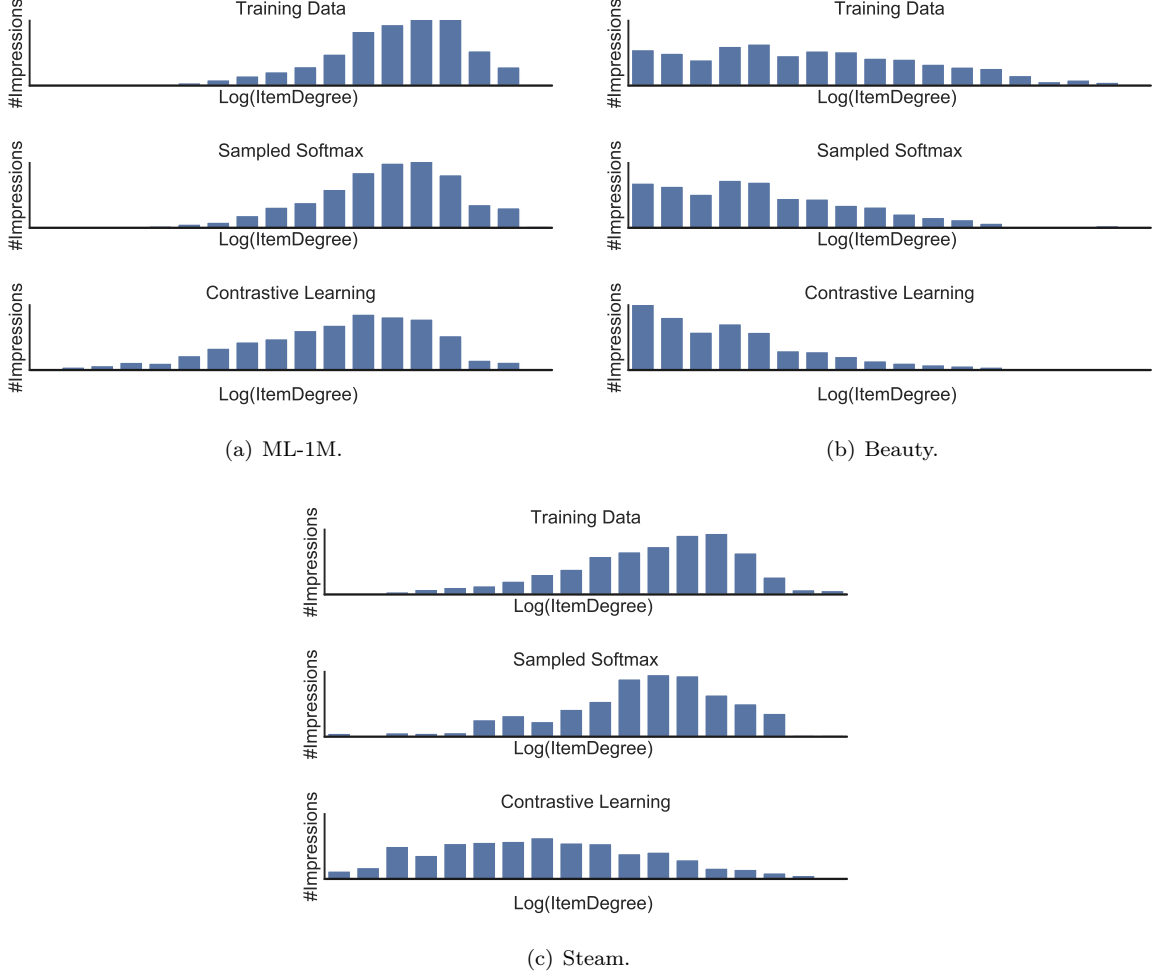


Figure 4: The total number of impressions of the items in a specific degree bucket vs. the logarithm of the corresponding degree. Sample softmax tends to faithfully fit the training data’s distribution, while CLRec tends to explore the previously under-explored items.

of negative sampling with sharing still uses the binary cross-entropy loss used by the original negative sampling implementation.

- Sampled softmax [21]: We use the sampled softmax implemented in Tensorflow [1], which subtracts the correction term (see Section 2) to ensure that the sampled loss is approximately optimizing the same loss as the full loss. We set the number of negative examples used by sample softmax per batch to be the same as the queue size used by CLRec.
- CLRec. See Section 2 for details. The batch size is 256 and the queue size is 2,560.

E Implementations of Complex Pretext Tasks

The implementation of CLRec that caches the computed results brings opportunities for efficiently implementing more advanced encoders that perform time-consuming operations on y , e.g. incorporating rich features of complex data types. With the help of the queue cache, we investigate a new type of self-supervised pretext task for training a recommender, which we call task u2u. In task u2u, x and y are both sequences from the same user, before and after a sampled timestamp, respectively. We use the same sequence encoder to encode x and y , but additionally add a fully connected layer to transform the vector representation of x produced by the sequence encoder. Intuitively, pre-training a recommender to solve task u2u may improve a recommender’s ability to make long-term prediction. We co-train the same encoders to solve both task u2u and the original u2i task where x and y are a sequence and the

sequence’s next click. Note that task u2i is still required, since we ultimately need the recommender to recommend items rather than sequences at serving time. We add the losses of the two tasks together, without introducing any parameter for weighting the two loss. The batch size is 256. We use one separate queue of size 2,560 for each task. We limit the sequence length of y in task u2u to be less than ten. We also investigate whether Momentum Contrast (MoCo) [16] may improve performance, and vary the momentum parameter in the range of $\{0.9, 0.99, 0.999, 0.9999\}$ and report the best result.

F Debiasing Effects on Public Datasets

To ensure reproducibility, we conduct the same qualitative analyses as described in Subsection 3.1.1 to demonstrate the debiasing effects of CLRec on the public benchmarks. We sample a sequence from each user in the training set as the input to the recommenders, and use the sampled sequences’ next immediate one clicks as the labels to predict. Each algorithm then retrieves top ten items for each sequence. The results are shown in Table 11 and Figure 4.

In Table 11, we report aggregate diversity of the items retrieved by the algorithms, as well as the aggregate diversity of the ground-truth next clicks. We can see that CLRec retrieves a more diverse set of items than sampled softmax. In other words, much more items will have a chance to be recommended after we reduce the bias in the training data.

In Figure 4, we visualize the distributions of the items retrieved by each algorithm, as well as the training data’s distribution. We can see that sample softmax tends to faithfully fit the training data’s distribution, while CLRec tends to explore the previously under-explored items.